Efficient Fixed-Offset GPR Scattering Analysis

Meincke, Peter; Chen, Xianyao

Published in:
Tenth International Conference on Ground Penetrating Radar

Publication date:
2004

Document Version
Publisher's PDF, also known as Version of record

Efficient Fixed-Offset GPR Scattering Analysis

Peter Meincke and Xian-Yao Chen
Ørsted·DTU, Electromagnetic Systems
Technical University of Denmark
Ørsteds Plads, Building 348
DK-2800 Kgs. Lyngby, Denmark
Email: pme@oersted.dtu.dk

Abstract— **The electromagnetic scattering by buried three-dimensional penetrable objects, as involved in the analysis of ground penetrating radar systems, is calculated using the extended Born approximation. The involved scattering tensor is calculated using fast Fourier transforms (FFT's). We incorporate in the scattering calculation the correct radiation patterns of the ground penetrating radar antennas by using their plane-wave transmitting and receiving spectra. Finally, we derive an efficient FFT-based method to analyze a fixed-offset configuration in which the location of the transmitting antenna is different for each receiving antenna position.**

I. Introduction

Electromagnetic scattering by buried objects is an essential component of the analysis of GPR systems. Purely numerical approaches, such as the finite difference time domain method [1] and integral equations combined with the method of moments (MOM) [2], [3], are often used for such scattering calculations. However, since many practical GPR scattering problems are electrically large, these numerical methods are usually too time and memory consuming for realistic simulations of such GPR configurations. Moreover, most GPR systems operate in a fixed-offset mode in which the transmitter and receiver more together, and a new scattering problem must be solved for each new receiver location. Hence, for such fixed-offset configurations several electrically large scattering problems are to be solved to simulate just one fixed-offset survey.

The extended Born approximation (EBA) is a nonlinear approximation for scattering calculations [4]. In the EBA, the inverse operator of the traditional volume electric field integral equation is approximated analytically. Hence, the EBA is less memory consuming and faster to calculate than a MoM solution because a full impedance matrix does not need to be inverted. Also, being a nonlinear approximation, the EBA is more accurate than the traditional first Born approximation, and almost as efficient to calculate. The EBA was modified to analyze scattering by buried objects by Dasgupta *et al.* [5], Yu and Carin [6], Tseng [7], and Cui *et al.* [8]. Their work involves replacing the free-space dyadic Green's function used in [4] by the one applicable for a half space. Also, the accuracy of the EBA for frequencies relevant for GPR was investigated by Troelsen *et al.* [9] and Dasgupta *et al.* [5].

In this paper we use the EBA to calculate the scattering by buried dielectric objects, as involved in the analysis of GPR systems. We include the correct radiation patterns of the GPR antennas by using their plane-wave transmitting and receiving spectra [10]. The fact that the presence of the air-soil interface impacts the radiation patterns of the antennas is accounted for by the transmitting and receiving spectra. Since the formulation is based on plane-wave expansions, it can be efficiently calculated using fast Fourier transforms (FFT's). With the formulas cast in a special form, we show that the fixed-offset configuration also can be efficiently analyzed with FFT's.

Throughout the paper the time factor $\exp(-i\omega t)$ is assumed and suppressed.

II. The Fixed-Offset GPR Configuration

The GPR configuration involving the planar air-soil interface is shown in Figure 1. A Cartesian xyz-coordinate system is introduced such that the xy-plane coincides with the interface and such that $z \geq 0$ is air and $z < 0$ is soil. The air has permittivity ε_0, permeability μ_0, and wavenumber $k_0 = \omega\sqrt{\mu_0\varepsilon_0}$. The soil has permittivity ε_1, conductivity σ_1, permeability μ_0, and wavenumber $k_1 = \sqrt{\omega^2\mu_0\varepsilon_1 + i\omega\mu_0\sigma_1}$. The position of the receiving antenna is $\mathbf{r}_r = x_r\hat{\mathbf{x}} + y_r\hat{\mathbf{y}} + z_r\hat{\mathbf{z}}$ with $z_r \geq 0$ and the position of the transmitting antenna is $\mathbf{r}_t = \mathbf{r}_r + \mathbf{r}_\Delta$ with $\mathbf{r}_\Delta = x_\Delta\hat{\mathbf{x}} + y_\Delta\hat{\mathbf{y}}$ being fixed. Below the air-soil interface, penetrable objects with support V_s are buried. The transmitting antenna is attached to a coaxial cable. In a

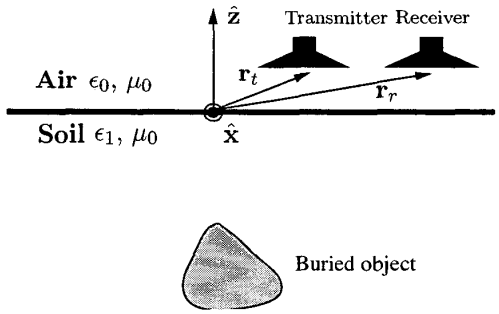

Fig. 1. The fixed-offset GPR configuration.

given reference plane in the cable, the voltage between the inner and outer conductor of the field propagating towards the antenna in the cable is V_t. The background field $\mathbf{E}^b$, defined as the field that would exist in the region $z < 0$ in the absence

of the objects, is then expressed in terms of the plane-wave transmitting spectrum $\mathbf{T}$ of the GPR antenna as [10]

$$\mathbf{E}^b(\mathbf{r}) = \frac{V_t}{(2\pi)^2}\int_{-\infty}^{\infty}\int \mathbf{T}(k_x,k_y)\exp(ik_x(x-x_r - x_\Delta)+k_y(y-y_r-y_\Delta)-\gamma_1 z])\,dk_x\,dk_y \quad (1)$$

where $z<0$ and $\mathbf{r}=x\hat{\mathbf{x}}+y\hat{\mathbf{y}}+z\hat{\mathbf{z}}$ is the position vector and $\gamma_1 = \gamma_1(k_x,k_y) = \sqrt{k_1^2-k_x^2-k_y^2}$ with $\mathrm{Im}\gamma_1 \geq 0$ is the z-component of the propagation vector in the soil.

III. Scattering by Buried Objects

The scattered field $\mathbf{E}^s$ in the soil can be approximated by the EBA as [4],

$$\mathbf{E}^s(\mathbf{r}) = i\omega\mu_0\int_{V_s}\bar{\mathbf{G}}(\mathbf{r},\mathbf{r}')\cdot\bar{\Gamma}(\mathbf{r}')\cdot\mathbf{E}^b(\mathbf{r}')O(\mathbf{r}')d^3\mathbf{r}' \quad (2)$$

where $z<0$, $\mathbf{r}'=x'\hat{\mathbf{x}}+y'\hat{\mathbf{y}}+z'\hat{\mathbf{z}}$, and $O(\mathbf{r})$ is the object function, describing the contrast in the electromagnetic properties from those of the background,

$$O(\mathbf{r}) = \sigma(\mathbf{r})-\sigma_1 - i\omega(\varepsilon(\mathbf{r})-\varepsilon_1). \quad (3)$$

Herein, $\varepsilon(\mathbf{r})$ and $\sigma(\mathbf{r})$ are the permittivity and conductivity distributions, respectively. Furthermore, $\bar{\mathbf{G}}(\mathbf{r},\mathbf{r}')$ in (2) is the dyadic Green's function for a homogeneous medium with wavenumber k_1 [11, p. 381].

$$\bar{\mathbf{G}}(\mathbf{r},\mathbf{r}') = \mathrm{P.V.}\left(\bar{\mathbf{I}}+\frac{\nabla\nabla}{k_1^2}\right)g(\mathbf{r},\mathbf{r}') - \frac{\bar{\mathbf{L}}}{k_1^2}\delta(\mathbf{r}-\mathbf{r}') \quad (4)$$

with P.V. referring to the principle value and $\bar{\mathbf{L}}$ depends on the shape of the chosen principle volume. Furthermore, $g(\mathbf{r},\mathbf{r}')$ is the usual scalar 3-D Green's function for a homogeneous medium,

$$g(\mathbf{r},\mathbf{r}') = \frac{\exp(ik_1|\mathbf{r}-\mathbf{r}'|)}{4\pi|\mathbf{r}-\mathbf{r}'|}. \quad (5)$$

By using the dyadic Green's function for a homogeneous medium, multiple interactions between the objects and the air-soil interface are neglected. This is a good approximation because of the loss in the soil [12]. The scattering tensor $\bar{\Gamma}$ in (2) is given by [4]

$$\bar{\Gamma}(\mathbf{r}) = \left[\bar{\mathbf{I}} - i\omega\mu_0\int_{V_s}\bar{\mathbf{G}}(\mathbf{r},\mathbf{r}')O(\mathbf{r}')d^3\mathbf{r}'\right]^{-1}. \quad (6)$$

The receiving antenna of the GPR is connected to a matched receiver through a coaxial cable with characteristic admittance Y_0. In a given reference plane in the cable, the voltage V between the inner and outer conductor of the field propagating away from the antenna in the cable is [10],

$$V(\mathbf{r}_r) = \frac{1}{(2\pi)^2}\int_{-\infty}^{\infty}\int \mathbf{R}(k_x,k_y)\cdot\mathbf{S}_1(k_x,k_y)\cdot\exp(i[k_x x_r+k_y y_r])\,dk_x\,dk_y \quad (7)$$

where $\mathbf{R}(k_x,k_y)$ is the plane-wave receiving spectrum of the GPR antenna, to be discussed below following (8), and $\mathbf{S}_1(k_x,k_y)$ is the plane-wave spectrum of the upward-propagating field $\mathbf{E}_1$ in the soil, determined by [13]

$$\mathbf{S}_1(k_x,k_y) = \frac{-\omega\mu_0}{2\gamma_1}\left(\bar{\mathbf{I}}-\frac{\mathbf{k}_1\mathbf{k}_1}{k_1^2}\right)\cdot[\widetilde{O\bar{\Gamma}\cdot\mathbf{E}^b}](\mathbf{k}_1) \quad (8)$$

where $\mathbf{k}_1 = k_x\hat{\mathbf{x}}+k_y\hat{\mathbf{y}}+\gamma_1\hat{\mathbf{z}}$ and $[\widetilde{O\bar{\Gamma}\cdot\mathbf{E}^b}]$ is the 3-D spatial Fourier transform of $O\bar{\Gamma}\cdot\mathbf{E}^b$.

The plane-wave receiving spectrum $\mathbf{R}(k_x,k_y)$ in (7) satisfies that $\mathbf{R}(k_x,k_y)\cdot\mathbf{k}_1 = 0$. For a reciprocal GPR antenna, the receiving spectrum is related to the transmitting spectrum $\mathbf{T}_r(k_x,k_y)$ of the receiving GPR antenna, defined as in (1), as [10]

$$\mathbf{R}(k_x,k_y) = \frac{\gamma_1}{\omega\mu_0 Y_0}\mathbf{T}_r(-k_x,-k_y). \quad (9)$$

The final expression for the output voltage V is obtained by inserting the plane-wave spectrum (8) into (7),

$$V(\mathbf{r}_r) = \frac{-\omega\mu_0}{8\pi^2}\int_{-\infty}^{\infty}\int\frac{1}{\gamma_1}\mathbf{R}(k_x,k_y)\cdot[\widetilde{O\bar{\Gamma}\cdot\mathbf{E}^b}](\mathbf{k}_1)\cdot\exp(i[k_x x_r+k_y y_r])\,dk_x\,dk_y \quad (10)$$

where the fact that $\mathbf{R}(k_x,k_y)\cdot\mathbf{k}_1 = 0$ has been applied. Since the derivation of the final expression (10) for the output voltage is based on plane-wave expansions, the calculation can be efficiently performed using FFT's. FFT's have been used previously by Liu *et al.* [14] to calculate the scattered field from the EBA in the 2-D free-space case, and by Tseng *et al.* in the 3-D half-space case. Indeed, the integrations over k_x,k_y in (10) can be calculated using 2-D FFT's. Also, the background field $\mathbf{E}^b$, determined from (1), can be calculated from 2-D FFT's for each value of z. Finally, the 3-D spatial Fourier transform $[\widetilde{O\bar{\Gamma}\cdot\mathbf{E}^b}]$ in (10) can be calculated using 3-D FFT's, or alternatively, from 2-D FFT's over x,y and subsequent integration over z. In either case it is assumed that the volume V_s is inside a grid of N non-overlapping and equal-sized boxes V_n.

IV. Calculating the Scattering Tensor

Two methods for calculating the scattering tensor $\bar{\Gamma}$ in (6) is now proposed. The starting point of both methods is to write the scattering tensor, evaluated at the center $\mathbf{r}_m$ of the m'th box, in convolutional form as

$$\bar{\Gamma}(\mathbf{r}_m) = \left[\bar{\mathbf{I}}-\frac{i\omega\mu_0}{k_1^2}\bar{\mathbf{N}}(\mathbf{r}_m)\right]^{-1} \quad (11)$$

with

$$\bar{\mathbf{N}}(\mathbf{r}_m) = \sum_n O(\mathbf{r}_n)\bar{\mathbf{P}}(\mathbf{r}_m-\mathbf{r}_n), \quad (12)$$

$$\bar{\mathbf{P}}(\mathbf{r}_m) = (k_1^2\bar{\mathbf{I}}+\nabla\nabla)\int_{V_0}g(\mathbf{r}_m,\mathbf{r}')\,d^3\mathbf{r}', \quad (13)$$

and V_0 is the box with center at the origin $\mathbf{r}_0$. The expression for $\bar{\mathbf{N}}$ in (12) is in a form suitable for FFT's.

In the first method $\bar{\mathbf{P}}$ in (13) is cast into a 2-D integral over the surface S_m of the m'th box, thus avoiding the singularity in the integrand of $\bar{\mathbf{P}}(\mathbf{r}_0)$ [13],

$$\begin{aligned}\bar{\mathbf{P}}(\mathbf{r}_m) = -\Big(&\hat{\mathbf{x}}H_m + \oint_{S_m} (\hat{\mathbf{x}}\nabla g(\mathbf{r}_m,\mathbf{r}')\cdot\hat{\mathbf{n}}' \\ &- \hat{\mathbf{x}}\cdot\nabla g(\mathbf{r}_m,\mathbf{r}')\hat{\mathbf{n}}')d^2\mathbf{r}'\Big)\hat{\mathbf{x}} \\ -\Big(&\hat{\mathbf{y}}H_m + \oint_{S_m} (\hat{\mathbf{y}}\nabla g(\mathbf{r}_m,\mathbf{r}')\cdot\hat{\mathbf{n}}' \\ &- \hat{\mathbf{y}}\cdot\nabla g(\mathbf{r}_m,\mathbf{r}')\hat{\mathbf{n}}')d^2\mathbf{r}'\Big)\hat{\mathbf{y}} \\ -\Big(&\hat{\mathbf{z}}H_m + \oint_{S_m} (\hat{\mathbf{z}}\nabla g(\mathbf{r}_m,\mathbf{r}')\cdot\hat{\mathbf{n}}' \\ &- \hat{\mathbf{z}}\cdot\nabla g(\mathbf{r}_m,\mathbf{r}')\hat{\mathbf{n}}')d^2\mathbf{r}'\Big)\hat{\mathbf{z}} \end{aligned} \tag{14}$$

where $H_m = 1$ if $m = 0$ and 0 otherwise. The dyadic $\bar{\mathbf{P}}$ in (14) can be determined by simply calculating three 2-D integrals and three 1-D integrals with scalar integrands.

In the second method, which is more efficient, the dyadic $\bar{\mathbf{P}}$ in (13) is calculated by inserting into (13) for $\bar{\mathbf{P}}$ the 3-D Fourier representation of $\bar{\mathbf{G}}(\mathbf{r}_m,\mathbf{r}')$,

$$\begin{aligned}\bar{\mathbf{G}}(\mathbf{r}_m,\mathbf{r}') = \frac{1}{(2\pi)^3}\int_{-\infty}^{\infty}\iiint \frac{\bar{\mathbf{I}} - \mathbf{k}_1\mathbf{k}_1/k_1^2}{k_x^2+k_y^2+k_z^2-k_1^2} \\ \cdot\exp(i[k_x(x_m-x')+k_y(y_m-y') \\ + k_z(z_m-z')])\,dk_x\,dk_y\,dk_z \end{aligned} \tag{15}$$

and evaluating analytically the integration over k_z. The resulting expression can be calculated by 2-D FFT's.

V. Fixed-Offset Configuration

The expression (10) for $V(\mathbf{r}_r)$, derived in Section III, is very inefficient for fixed-offset configurations: First, since the transmitting and receiving antennas are at a fixed offset, the background field $\mathbf{E}^b$ changes when the radar is moved. Therefore, $\mathbf{E}^b$ needs to be recalculated for each new location of the receiving antenna. Second, when (10) is calculated using FFT's, the output voltage is simultaneously determined for several observation points in a square grid, but only the one corresponding to the receiving antenna position is needed. In the following, a efficient method is derived to deal with the considered fixed-offset configuration.

To derive the efficient method, insert first the expression (1) for the background field $\mathbf{E}^b$, with k_x, k_y replaced by k_x', k_y', into the relation (10) for the output voltage. Second, inspired by the procedure in [12], interchange the integrations over k_x, k_y and k_x', k_y' and carry out the substitutions $k_x'' = k_x - k_x'$ and $k_y'' = k_y - k_y'$. The result is [13]

$$\begin{aligned}V(\mathbf{r}_r) = \int_{-\infty}^{\infty}\int F(k_x'',k_y'') \\ \cdot\exp\left(i\left[k_x''x_r + k_y''y_r\right]\right)dk_x''\,dk_y'' \end{aligned} \tag{16}$$

with

$$\begin{aligned}F(k_x'',k_y'') = \int_{z'\in V_s} &\bar{\mathbf{H}}(k_x'',k_y'',z') \\ &: \bar{\mathbf{S}}(k_x'',k_y'',z')\,dz', \end{aligned} \tag{17}$$

$$\begin{aligned}\bar{\mathbf{H}}(k_x'',k_y'',z') = \iint_{(x',y')\in V_s} &O(\mathbf{r}')\bar{\Gamma}(\mathbf{r}') \\ &\cdot\exp\left(-i\left[k_x''x' + k_y''y'\right]\right)dx'\,dy', \end{aligned} \tag{18}$$

$$\begin{aligned}\bar{\mathbf{S}}(k_x'',k_y'',z') = \int_{-\infty}^{\infty}\int &\mathbf{C}_1(k_x,k_y,z')\mathbf{C}_2(k_x''-k_x, \\ &k_y''-k_y,z')\,dk_x\,dk_y. \end{aligned} \tag{19}$$

with

$$\mathbf{C}_1(k_x,k_y,z') = \frac{-\omega\mu_0 V_t}{32\pi^4\gamma_1}\mathbf{R}(k_x,k_y)\exp\left(-i\gamma_1 z'\right), \tag{20}$$

$$\begin{aligned}\mathbf{C}_2(k_x,k_y,z') = &\exp\left(i\left[k_x x_\Delta + k_y y_\Delta - \gamma_1 z'\right]\right) \\ &\cdot\mathbf{T}(-k_x,-k_y). \end{aligned} \tag{21}$$

The double product : in (17) is defined as $(\mathbf{AB}) : (\mathbf{CD}) = \mathbf{A}(\mathbf{B}\cdot\mathbf{C})\mathbf{D}$.

These final equations for the output voltage can be calculated efficiently with FFT's. In particular, the integrations over k_x'', k_y'' in the expression (16) for V can be determined for all needed receiver locations using one single 2-D FFT. The integrations over k_x, k_y of the nine components of the dyadic $\mathbf{C}_1(k_x,k_y,z')\mathbf{C}_2(k_x''-k_x,k_y''-k_y,z')$ in the expression (19) for $\bar{\mathbf{S}}$ are in convolutional form and therefore, for a fixed z', $\bar{\mathbf{S}}(k_x'',k_y'',z')$ can be calculated for all needed values of k_x'' and k_y'' using 2-D FFT's. Moreover, the relation for $\bar{\mathbf{H}}$ can for each z' be calculated by 2-D FFT's for all needed values of k_x'', k_y''.

We will now discuss how to use the FFT to do the above-mentioned calculations. The functions $\mathbf{C}_1$ and $\mathbf{C}_2$ in (20) and (21) contain the factor $\exp(-i\gamma_1 z')$ which is exponentially decaying for $k_x^2 + k_y^2 > \mathrm{Re}\,k_1^2$. Hence, $\mathbf{C}_1$ and $\mathbf{C}_2$ are spatially band limited with the bandwidth $k_{\max}$ determined by requiring that $\exp(-\sqrt{k_{max}^2 - k_1^2}|z'|)$, with $k_{\max} > \mathrm{Re}\,k_1$, is sufficiently small. The integrations over k_x, k_y in (19) extend over the ranges $-k_{\max} < k_x < k_{\max}$ and $-k_{\max} < k_y < k_{\max}$. Equations (17) and (19) then show that the functions $F(k_x'',k_y'')$ and $\bar{\mathbf{S}}(k_x'',k_y'',z')$ are band limited with the bandwidth $2k_{\max}$. Hence, the grid, on which the output voltage (16) is calculated using FFT's, has the spacing $\Delta x_r = \Delta y_r = \pi/(2k_{\max})$.

Acknowledgment

The Danish Technical Research Council is acknowledged for supporting this work.

References

[1] A. Taflove, *Computational Electrodynamics. The Finite-Difference Time-Domain Method.* Artech Hourse, Boston, 1995.

[2] K. A. Michalski and D. Zheng, "Electromagnetic scattering and radiation by surfaces of arbitrary shape in layered media. Part I: Theory," *IEEE Trans. Antennas Propagat.*, vol. 38, pp. 335–344, Mar. 1990.

[3] E. Jørgensen, O. S. Kim, P. Meincke, and O. Breinbjerg, "Higher-order hierarchical discretization scheme for surface integral equations for layered media," *IEEE Trans. Geosci. Remote Sensing*, Apr. 2004, to appear.

[4] T. M. Habashy, R. W. Groom, and B. R. Spies, "Beyond the Born and Rytov approximations: a nonlinear approach to electromagnetic scattering," *Journal of Geophysical Research*, no. B2, pp. 1759–1775, Feb. 1993.

[5] N. Dasgupta, N. Geng, T. Dogaru, and L. Carin, "On the extended-Born technique for scattering from buried dielectric targets," *IEEE Trans. Antennas Propagat.*, vol. 47, no. 11, pp. 1739–1742, Nov. 1999.

[6] T. J. Yu and L. Carin, "Analysis of the electromagnetic inductive response of a void in a conducting-soil background," *IEEE Trans. Geosci. Remote Sensing*, vol. 38, no. 3, pp. 1320–1327, May 2000.

[7] H.-W. Tseng, K. H. Lee, and A. Becker, "3D interpretation of electromagnetic data using a modified extended Born approximation," *Geophysics*, vol. 68, no. 1, pp. 127–137, jan.feb 2003.

[8] T. J. Cui, W. C. Chew, A. A. Aydiner, and Y. H. Zhang, "Fast-forward solvers for the low-frequency detection of buried dielectric objects," *IEEE Trans. Geosci. Remote Sensing*, vol. 41, no. 9, pp. 2026–2036, Sept. 2003.

[9] J. Troelsen, P. M. Johansen, and O. Breinbjerg, "An investigation of the extended Born approximation at high frequencies for ground penetrating radar imaging," in *Proceedings of the International Conference on Electromagnetics in Advanced Applications*, Torino, Italy, Sept. 1999.

[10] P. Meincke and T. B. Hansen, "Plane-wave characterization of antennas close to a planar interface," *IEEE Trans. Geosci. Remote Sensing*, 2004, to appear.

[11] W. C. Chew, *Waves and Fields in Inhomogeneous Media*. IEEE Press, 1995.

[12] T. B. Hansen and P. Meincke, "Scattering from a buried circular cylinder illuminated by a 3-D source," *Radio Science*, vol. 37, pp. 4–1 – 4–23, Mar. 2002.

[13] P. Meincke, X.-Y. Chen, and O. Kim, "Scattering analysis of ground penetrating radar systems using the extended Born approximation," submitted to *IEEE Trans. Antennas Propagat.*

[14] Q. H. Liu, Z. Q. Zhang, and X. M. Xu, "The hybrid extended Born approximation and CG-FFT method for electromagnetic induction problems," *IEEE Trans. Geosci. Remote Sensing*, vol. 39, no. 2, pp. 347–354, Feb. 2001.